Downregulation and delayed induction of photosynthesis by coordinated transcriptomic changes in response to sink-source imbalance

Daisuke Sugiura[1], Yui Ozawa[1], Aiko Tanaka[1], and Takamasa Suzuki[2]

[1]Nagoya Daigaku
[2]Chubu Daigaku

February 21, 2023

Abstract

Sink-source imbalance causes accumulation of non-structural carbohydrates (NSCs) and photosynthetic downregulation. Despite numerous studies, however, it remains unclear whether NSCs accumulation or N deficiency more directly decreases steady-state maximum photosynthesis and photosynthetic induction, as well as underlying gene expression profiles. We evaluated the relationship between photosynthetic capacity and NSCs accumulation induced by cold-girdling, sucrose feeding, and low nitrogen treatment in *Glycine max* and *Phaseolus vulgaris*. In *G. max*, changes in transcriptome profiles were further investigated focusing on physiological processes of photosynthesis and NSCs accumulation. NSCs accumulation decreased maximum photosynthetic capacity and delayed photosynthetic induction in both species. In *G. max*, such photosynthetic downregulation was explained by coordinated downregulation of photosynthetic genes involved in Calvin cycle, Rubisco activase, photochemical reactions, and stomatal opening. Furthermore, sink-source imbalance may have triggered a change in the balance of sugar-phosphate translocators in chloroplast membranes, which may have promoted starch accumulation in chloroplasts. Our findings provided an overall picture of the photosynthetic downregulation and NSCs accumulation in *G. max*, demonstrating that the photosynthetic downregulation is triggered by NSCs accumulation and cannot be explained simply by N deficiency.

Hosted file

`Manuscript with Ref PCE.docx` available at https://authorea.com/users/588371/articles/625609-downregulation-and-delayed-induction-of-photosynthesis-by-coordinated-transcriptomic-changes-in-response-to-sink-source-imbalance

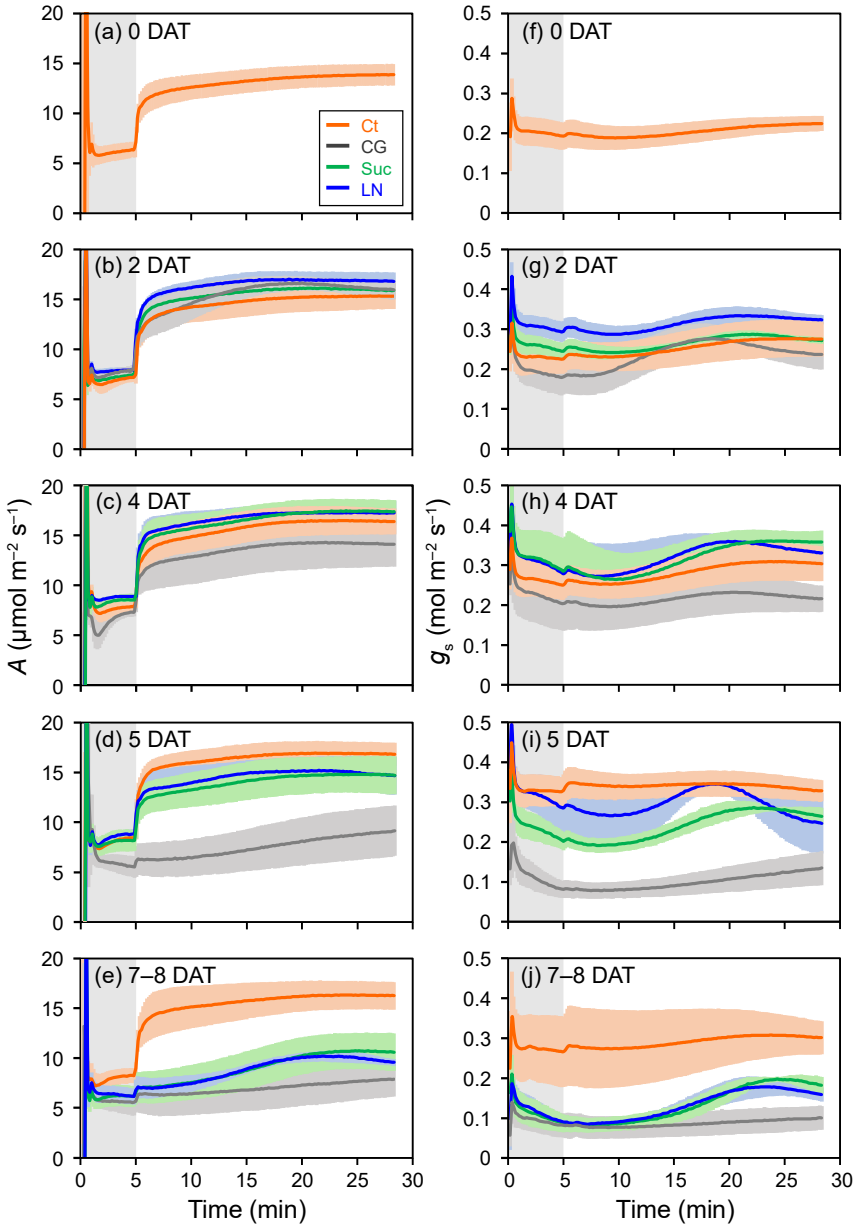

Fig. 1 Temporal response of net CO_2 assimilation (A) and stomatal conductance (g_s) to a step change in PPFD from 200 (shaded area) to 1000 (unshaded area) μmol m^{-2} s^{-1} in *G. max*. (a, f) 0 day after treatments (DAT), (b, g) 2 DAT, (c, h) 4 DAT, (d, i) 5 DAT, (e, j) 7–8 DAT. Orange, grey, green, and blue lines indicate control (Ct), cold-girdling (CG), sucrose feeding (Suc), and low nitrogen (LN) treatments, respectively. Values are mean ± SD with a measurement interval of 10 seconds obtained from Exp. 1–3 (n=4–12).

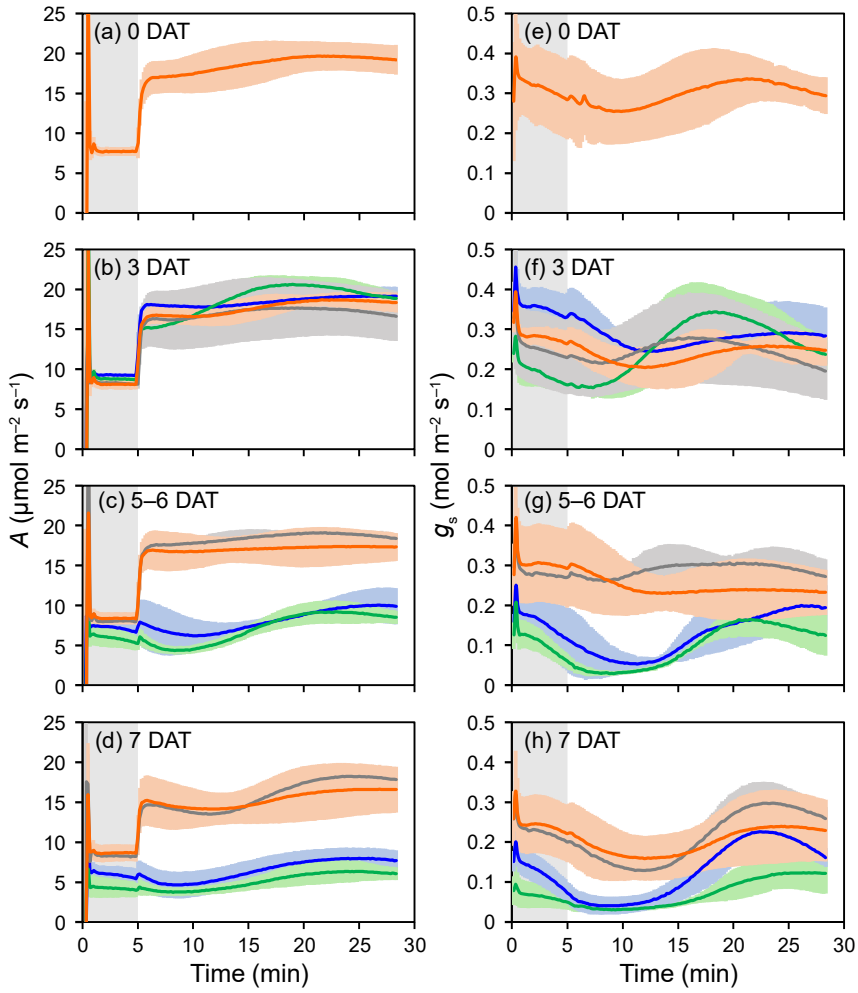

Fig. 2 Temporal response of net CO_2 assimilation (A) and stomatal conductance (g_s) to a step change in PPFD from 200 (shaded area) to 1000 (unshaded area) μmol m^{-2} s^{-1} in *P. vulgaris*. (a, e) 0 day after treatments (DAT), (b, f) 2 DAT, (c, g) 5~6 DAT, (d, h) 7 DAT. Orange, grey, green, and blue lines indicate control (Ct), cold-girdling (CG), sucrose feeding (Suc), and low nitrogen (LN) treatments, respectively. Values are mean ± SD with a measurement interval of 10 seconds obtained from Exp. 1–2 (n=4–8).

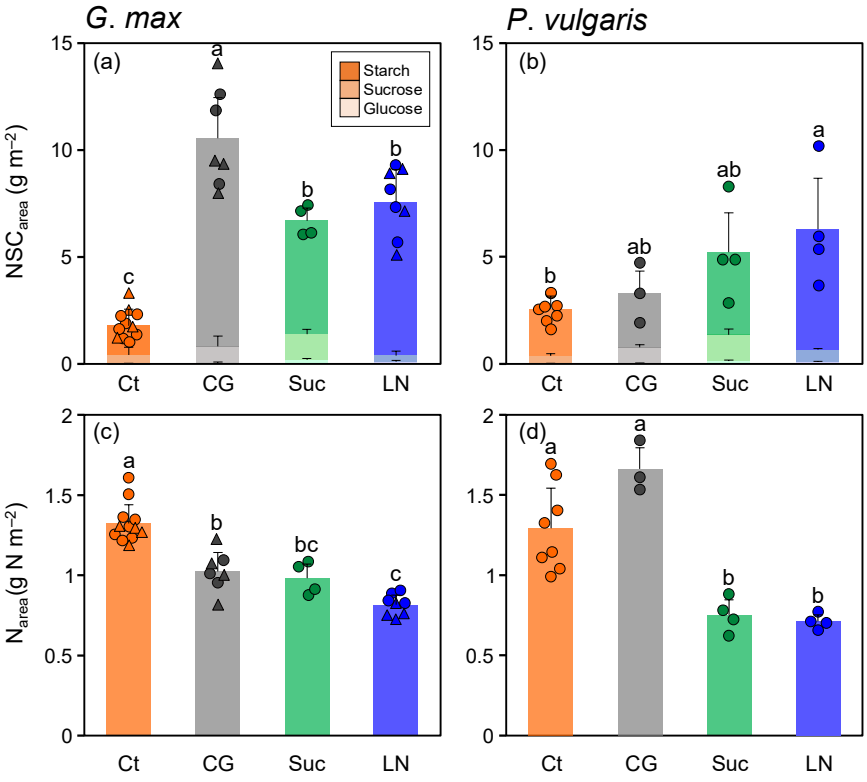

Fig. 3 Nonstructural carbohydrate (NSC_{area}) and leaf nitrogen content per area (N_{area}) in the primary leaves of *G. max* and *P. vulgaris* on 7–8 days after treatments (DAT). (a, c) *G. max* and (b, d) *P. vulgaris*. Orange, grey, green, and blue bar indicate control (Ct), cold-girdling (CG), sucrose feeding (Suc), and low nitrogen (LN) treatments, respectively. NSC_{area} is expressed as sum of starch, sucrose, and glucose. Triangle represents data of *G. max* in Exp. 3. Bars are mean + SD obtained from Exp. 1–3 (n=4–12). Different lower-case letters indicate significant differences among treatments (Tukey's test, $P < 0.05$).

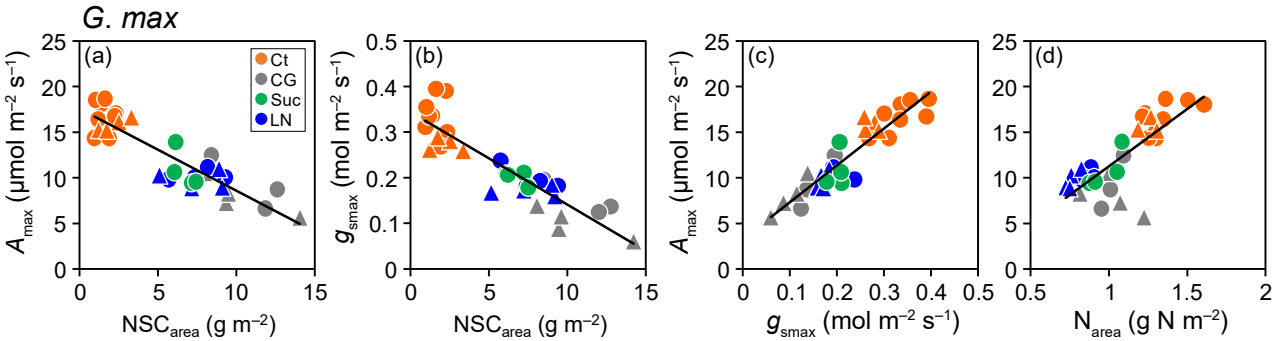

Fig. 4 Relationships between photosynthetic traits (A_{max} and g_{smax}), nonstructural carbohydrate (NSC_{area}), and leaf nitrogen content per area (N_{area}) in the primary leaves of *G. max* on 7–8 days after treatments (DAT). Orange, grey, green, and blue symbols indicate control (Ct), cold-girdling (CG), sucrose feeding (Suc), and low nitrogen (LN) treatments, respectively. Triangle represents data of *G. max* in Exp. 3. Values of R^2 are (a) 0.77, (b) 0.71, (c) 0.86, (d) 0.61 ($P < 0.01$).

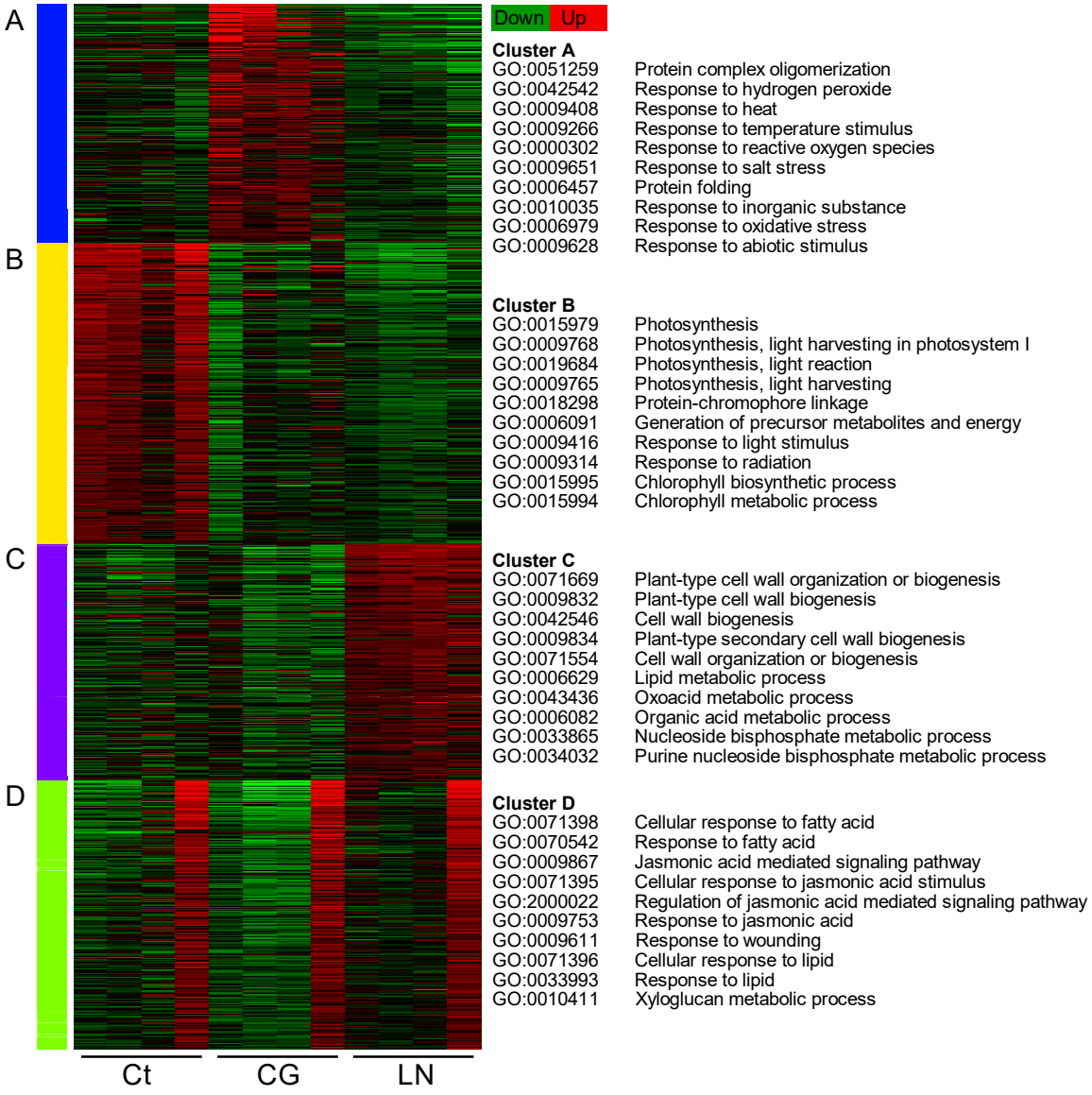

Fig. 5 K-means clustering and gene ontology (GO) enrichment analysis from transcriptome data of *G*. *max* obtained in Exp. 3. Heat map shows up- (red) and down- (green) regulated genes in control (Ct), cold-girdling (CG), and low nitrogen (LN) (n = 4). 2000 genes were grouped into 4 clusters, each of which include 442 (Cluster A), 557 (Cluster B), 473 (Cluster C), and 508 genes (Cluster D) (Supplementary Table X). Top 10 GO biological processes were shown for each cluster.

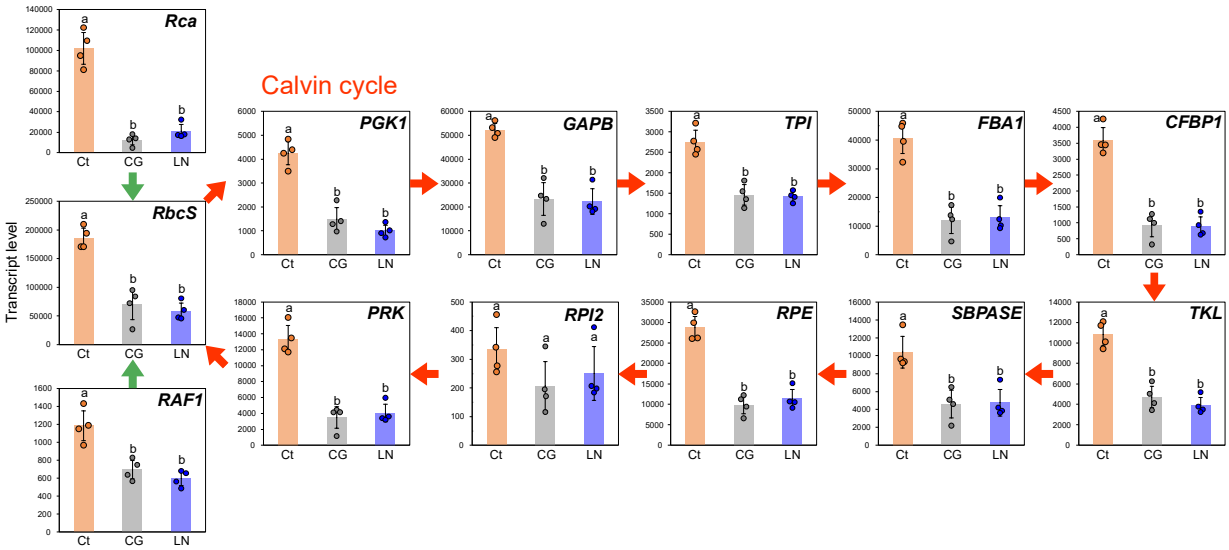

Fig. 6 Expression of key genes in the Calvin cycle in response to cold-girdling (CG) and low nitrogen (LN). Data are obtained from transcriptome data of *G. max* in Exp. 3. Transcript levels of genes annotated with Arabidopsis gene ID are calculated as the total read counts of duplicated genes of *G. max* (Supplementary Table 3). RCA is Rubisco activase that facilitates Rubisco activation, and RAF is Rubisco accumulation factor required for assembly and stability of Rubisco. PRK is responsible for the regeneration of RuBP. Bars are mean ± SD (n=4). Different lower-case letters indicate significant differences among treatments (Tukey's test, $P < 0.05$).

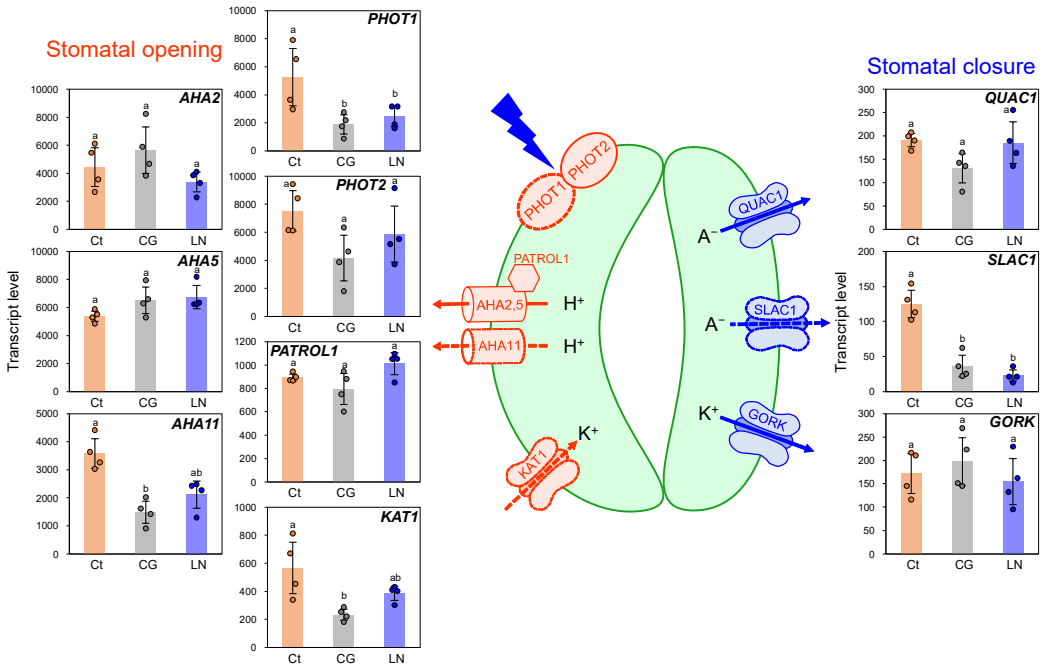

Fig. 7 Changes in expression of genes promoting stomatal opening or closure in response to cold-girdling (CG) and low nitrogen (LN). Data are obtained from transcriptome data of *G. max* in Exp. 3. Transcript levels of genes annotated with Arabidopsis gene ID are calculated as the total read counts of duplicated genes of *G. max* (Supplementary Table 7). PHOT1 and PHOT2 are blue-light receptors, and PATROL1 is involved in the localization of H^+-ATPase. KAT1 and GORK are inward and outward potassium (K^+) channels, respectively, and QUAC1 and SLAC1 are outward anion (A^-) channels. Bars are mean ± SD (n=4). Different lower-case letters indicate significant differences among treatments (Tukey's test, $P < 0.05$).

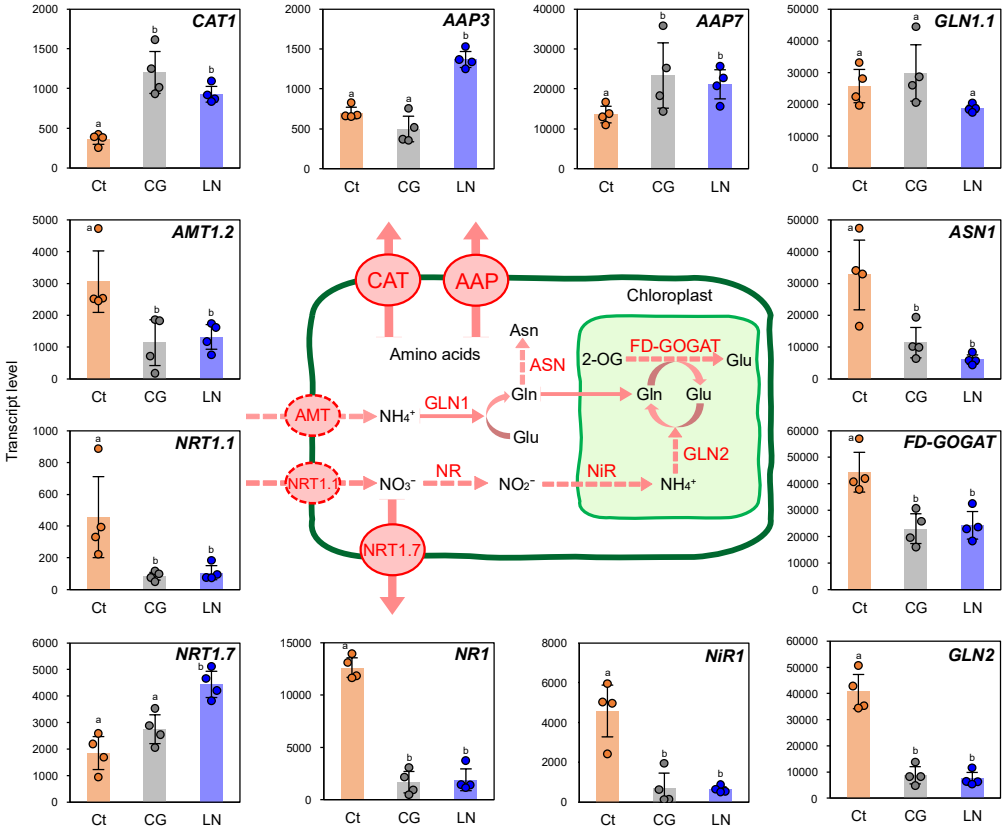

Fig. 8 Changes in expression of gene involved in nitrogen assimilation in response to cold-girdling (CG) and low nitrogen (LN). Data are obtained from transcriptome data of *G. max* in Exp. 3. Transcript levels of genes annotated with Arabidopsis gene ID are calculated as the total read counts of duplicated genes of *G. max* (Supplementary Table 8). NRT and AMT are NO_3^- and NH_4^+ transporter, respectively, where NRT1.7 is responsible for phloem loading of NO_3^-. NR and NiR are nitrate and nitrite reductase, respectively. GLN, FD-GOGAT, and ASN are glutamine (Gln), glutamate (Glu), and asparagine (Asn) synthase, respectively. CAT and AAP are cationic and neutral amino acid transporters, respectively. Bars are mean± SD (n=4). Different lower-case letters indicate significant differences among treatments (Tukey's test, $P < 0.05$).

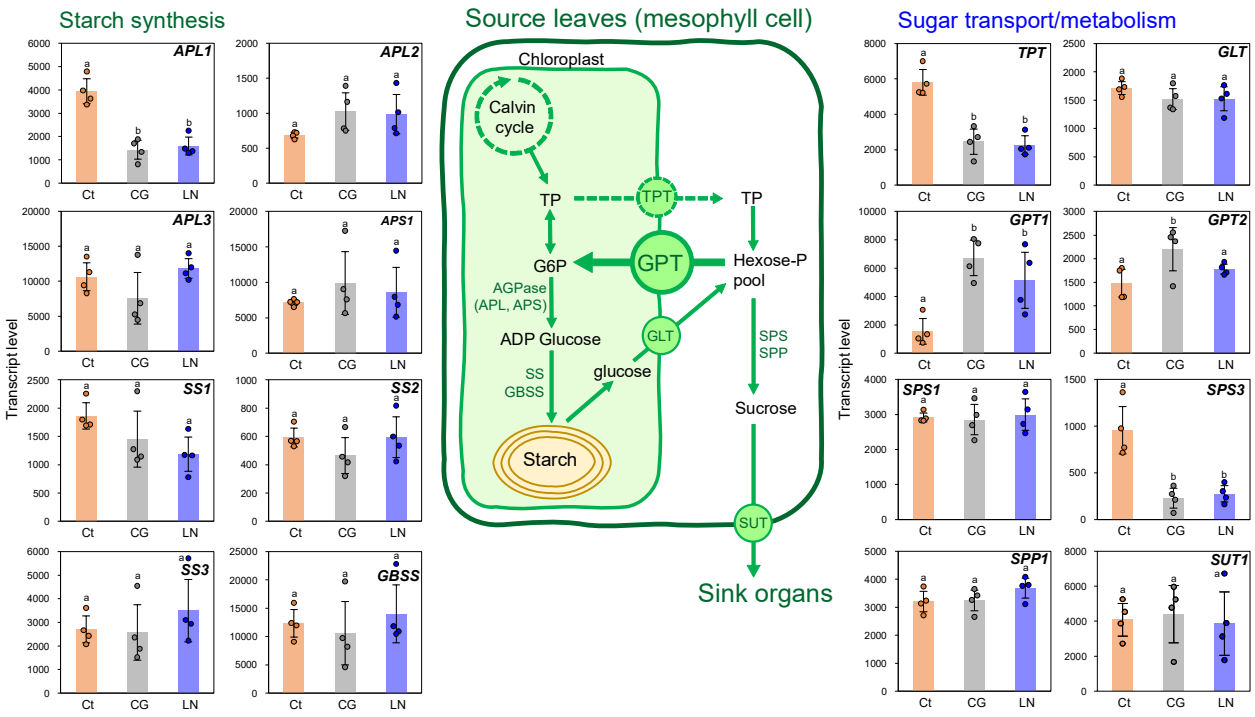

Fig. 9 Changes in expression of gene involved in starch synthesis and sugar transport/metabolism in response to cold-girdling (CG) and low nitrogen (LN). Data are obtained from transcriptome data of *G. max* in Exp. 3. Transcript levels of genes annotated with Arabidopsis gene ID are calculated as the total read counts of duplicated genes of *G. max* (Supplementary Tables 9-11). APL and APS are large and small subunits of ADP glucose pyrophosphorylase (AGPase), respectively. SS and GBSS are soluble and granule bound starch synthases, respectively. TPT and GLT export triose phosphate (TP) and glucose from the chloroplast to the cytosol, respectively. GPT transport glucose-6-phosphate (G6P) from the cytosol to the chloroplast. SPS and SPP play a major role in sucrose synthesis, and SUT is sucrose transporter. Bars are mean± SD (n=4). Different lower-case letters indicate significant differences among treatments (Tukey's test, $P < 0.05$).